

## Three-Level Inverter Performance Using Adaptive Neuro-Fuzzy Based Space Vector Modulation

G. Durgasukumar (Corresponding author)  
Research scholar, Department of Electrical Engg, IIT Roorkee  
Roorkee, India-247667  
Tel: 91-9760522273 E-mail: durgasukumar@gmail.com

M.K.Pathak  
Department of Electrical Engg, IIT Roorkee  
Roorkee, India-247667  
E-mail: mukesfee@iitr.ernet.in

### Abstract

Space vector modulation is an optimal pulse width modulation technique in variable speed drive application. This paper presents Adaptive Neuro-fuzzy based space vector modulation technique for a three level inverter. It uses hybrid learning algorithm (combination of back propagation and least square methods) for training due to this the required training error is obtained with less number of epoches compared to other techniques like Neural, fuzzy etc. The proposed scheme uses the d-axis and q-axis voltages information at the input side and the corrected two-level duty ratios for switching pulses, two-level index are generated as output. The performance measure in-terms of the total harmonic distortion (*THD*) of inverter line-line voltage has been evaluated with Adaptive Neuro-fuzzy based system is compared with the conventional based SVM method.

**Keywords:** Adaptive Neuro-Fuzzy inference system (ANFIS), three-level inverter. Two-level inverter, Space vector modulation (SVM), Total harmonic distortion (THD)

### 1. Introduction

Inverter is an electrical device that produces AC output voltage from a DC supply voltage. The converted AC can be at any required voltage and frequency with the use of appropriate switching and control circuits. The performance of inverter is mainly depends on the switching operation. As a result, number of pulse width modulation strategies has been developed and studied (Attainese.et.al.2007, Kwasinski. et.al.2003 and Wenxi et.al. 2008). In all these strategies, space-vector modulation (SVM) stands out because it reduces the harmonic content and offers significant flexibility to optimize switching waveforms. But the disadvantage of SVM is it requires complex online computation that limits the switching frequency of inverter.

In order to use high switching frequency power semiconductor devices (IGBTs) effectively, the operating frequency of SVM has to be increased. But practically DSP based conventional SVM fails when the switching frequency increases. This problem can be overcome by using techniques like neural, fuzzy, Neuro-fuzzy etc (Anshuman. et.al. 2005). A neural network based SVM is implemented and compared with the conventional DSP based SVM (Pinto. et.al.2000 and Mondal. et.al.2002). In this, ANN based SVM performance is deteriorated when compared to the conventional SVM. A neural network based SVM for different architectures and different switching frequencies have been studied ( Muthuramalingam. et.al. 2005). These discussed SVM techniques takes much time to train and total harmonic distortions (THD) obtained are more compared to the conventional method. The ANFIS method takes less time to train and gives better performance compared to other artificial intelligence methods due to its hybrid learning algorithm (Jyh-Shing Roger Jang.et.al.1993).

This paper describes ANFIS based SVM implementation of a two level voltage fed inverter. In Section 2, SVM theory of two-level inverter and three-level inverter is presented. ANFIS principle, architecture and ANFIS based SVM procedure is described In Section 3. Results of ANFIS based SVM and its comparison with conventional based SVM is presented in the Section 4. Concluding remarks are stated in section 5. Simulation studies are carried out using 3-Phase, 3hp, 400V, 50Hz, and 1480RPM induction motor.

## 2. Space vector modulation for three-level inverter

A three-level space-vector diagram can be decomposed into six space-vector diagrams of two-level. The space vector diagram three-level inverter and its corresponding two level hexagons are shown in Figure 1(a) and 1(b).

A three-level space-vector plane is transformed to the two-level space-vector plane by using the two steps

- 1) From the location of a given reference voltage and selected hexagon make a translation of the reference vector towards the centre of the hexagon.
- 2) The original reference voltage vector has to be subtracted by the amount of the center voltage vector of the selected hexagon.

From the location of a reference voltage and selected hexagon, if the reference voltage vector is in the regions that are overlapped by adjacent small hexagons then the space vector diagram can have multiple values. Once the value is obtained, the origin of a reference voltage vector is changed to the center of selected hexagon. This is obtained by subtracting the vector of the selected hexagon from the original reference vector of the three-level space vector diagram. Figure 2 represents the change of original reference voltage vector ( $V_{ref}$ ) from three-level to two-level ( $V^{2*}$ ).

After changing the reference vector the effective times are calculated in a similar manner of two-level inverter as

$$T_1 = \frac{V^{2*} T_s}{V_{dc} \cdot \frac{2}{3}} \cdot \frac{\sin\left(\frac{\pi}{3} - \alpha\right)}{\sin\frac{\pi}{3}} \quad (1)$$

$$T_2 = \frac{V^{2*} T_s}{V_{dc} \cdot \frac{2}{3}} \cdot \frac{\sin(\alpha)}{\sin\frac{\pi}{3}}, \quad (2)$$

$$T_0 = T_s - T_1 - T_2 \quad (3)$$

Where  $V^{2*}$  is the corrected reference voltage of two level.

The d and q components of the reference voltage  $V^{2*}$  is given in Table 1.

In order to generate two-level duty ratios independent of sampling time ( $T_s$ ) for the Adaptive Neuro-Fuzzy system the above equations are considered as

$$D_1 = M \cdot \frac{\sin\left(\frac{\pi}{3} - \alpha\right)}{\sin\left(\frac{\pi}{3}\right)} \quad (4)$$

$$D_2 = M \cdot \frac{\sin(\alpha)}{\sin\left(\frac{\pi}{3}\right)} \quad (5)$$

$$D_0 = 1 - (D_1 + D_2) \quad (6)$$

Where  $D_1$  is the duty cycle of switching vector that lags  $V_{ref}$

$D_2$  is the duty cycle of switching vector that leads  $V_{ref}$

$D_0$  is the duty cycle of zero switching vector.

The generated duty cycles are multiplied with the respective six sectors switching states, depending upon the sector number. The duty cycles obtained for the sector-1 is given by equations (7) and (8). For other sectors the values are calculated in similar method. As the null state is shared equally between  $V_0$  and  $V_7$  switching states, the value of each switching state is considered as 0.5. A two-level inverter space vector diagram with eight different switching states ( $V_0$ - $V_7$ ) represented in Figure 3.

Sector 1:

Turn on duty cycles

$$\begin{bmatrix} S_1 \\ S_3 \\ S_5 \end{bmatrix} = \begin{bmatrix} D_1 + D_2 + 0.5D_0 \\ D_2 + 0.5D_0 \\ 0.5D_0 \end{bmatrix} \quad (7)$$

Turn off duty cycles

$$\begin{bmatrix} S_2 \\ S_4 \\ S_6 \end{bmatrix} = \begin{bmatrix} D_1 + D_2 + 0.5D_0 \\ 0.5D_0 \\ D_1 + 0.5D_0 \end{bmatrix} \quad (8)$$

In Figure 4, the relationship between the effective duty cycles and the actual gating pattern is presented when the reference vector is located in the Sector-1. In this case, the  $V_1$  vector is applied to the inverter during  $D_1$  interval and  $V_2$  vector is applied during  $D_2$  interval. In the three phase symmetrical modulation method, the zero sequence voltage vectors is distributed symmetrically in one sampling period to reduce the ripple. Thus, in general, the switching sequence is given by 0-1-2-7-7-2-1-0 within two sampling periods. With the point of view of the upper switching devices of one inverter leg, the former sequence (0-1-2-7 sequence) is called 'ON' sequence, and the latter (7-2-1-0) is called 'OFF' sequence.

The generated duty cycles are compared with the up/down counter that is generated by the required sampling period. From the obtained time interval values switching pulses are generated using the relay circuit.

The desired corrected equalent two-level switching states are converted to three-level switching states by comparing the three-level switching states with conventional two-level switching states of selected hexagon and using the two-level index. A two-level index gives the hexagon number in which hexagon the reference vector is located. The conversion of two-level switching states into three-level switching states are shown in Figure 5.

### 3. ANFIS based space vector modulation

#### 3.1 Model of Adaptive neuro fuzzy controller for two-level switching pulses and Two-level index

The algorithm of proposed ANFIS controller that generates switching pulses and Two-level index is based on d-axis voltage  $V_{ds}$  and q-axis voltage  $V_{qs}$ . The corresponding typical Adaptive Neuro-fuzzy structure is shown in Figure 6.

From the first order Sugeno Fuzzy model, a typical rule set with two inputs  $V_{ds}$  and  $V_{qs}$  with responses  $f_1, f_2, \dots, f_n$  can be given in generalized form as

Rule: if ( $V_{ds}$  is  $M_i$ ) and ( $V_{qs}$  is  $M_j$ ) then

$$f_n = p_n V_{ds} + q_n V_{qs} + r_n \quad (9)$$

where  $n=1,2,\dots$  and  $i,j=1,2,\dots$  respectively

Where  $p_n, q_n, r_n$  are the linear parameters and  $M_i$  and  $M_j$  are non linear parameters.

The system architecture consists of five layers namely Fuzzy layer, product layer, normalized layer, defuzzification layer and total output layer.

**Layer 1:** It is fuzzy layer in which  $V_{ds}$  and  $V_{qs}$  are the inputs for each set of nodes  $M_1$  to  $M_5$  respectively. Where  $M_1$  to  $M_5$  are the linguistic labels used in fuzzy theory to define membership functions. The membership functions taken are bell shaped with maximum equal to 1 and minimum equal to 0. Every node in this layer is called as adoptive node and the parameters in this layer are called premise (Precondition) parameters.

The membership relation between the output and the input functions of this layer is expressed as

$$O'_{1i} = \mu M_i(V_{ds}) \quad i=1,2,\dots,5 \quad (10)$$

$$O'_{1j} = \mu M_j(V_{qs}) \quad j=1,2,\dots,5 \quad (11)$$

Where  $O'_{1i}$  and  $O'_{1j}$  denote the output of the nodes in the first layer

$\mu M_i$  and  $\mu M_j$  denote the membership functions of the layer

Bell shape membership function can be expressed using three parameters and can given as

$$F(x; a,b,c) = \frac{1}{1 + \left| \frac{x-c}{a} \right|^{2b}} \quad (12)$$

Where the parameter  $a$  and  $b$  vary the width of curve and the parameter  $c$  locates the center of the curve. The parameter  $b$  should be positive.

**Layer 2:** The output of every node in layer 2 is the product of all the incoming signals. Each node output represents the firing strength of a rule. A fuzzy rule neuron receives inputs from the previous layer that represent fuzzy sets in the rule antecedents. If there are multiple inputs to a neuron in this layer, the conjunction of the rule antecedents is evaluated by the fuzzy operation, intersection. This operation can also be used to combine multiple inputs to a fuzzy rule neuron. The total number of rules is 25 in this layer.

$$O'_2 = \mu M_i(V_{ds}) \text{AND} \mu M_j(V_{qs}) \quad (13)$$

**Layer 3:** It is a fixed node and it calculates the ratio of the  $i^{\text{th}}$  rule activation level to that of all activation levels. Neurons in this layer represent fuzzy sets used in the consequent of the fuzzy rules. An output membership neuron receives inputs from the previous layer neurons and combines them using the fuzzy operation, union. Therefore, the normalized firing strength computed can be given as

$$O'_3 = \frac{O_{2i}}{\sum_i O_{2i}} \quad i=1,2,\dots \quad (14)$$

**Layer 4:** It is an adaptive node and calculates the contribution of  $i^{\text{th}}$  rule towards the overall output. i.e., defuzzification process of fuzzy system (using weighted average method) is obtained. The output of a Neuro-fuzzy system is crisp, and thus, a combined output fuzzy set must be defuzzified. The node function can be expressed as

$$O'_4 = O'_3 \sum_{i=1}^p p_i V_{ds} + q_i V_{qs} + r_i \quad i=1,2,\dots,p \quad (15)$$

Where parameters  $p_1, p_2, \dots, p_p, q_1, q_2, \dots, q_p$  and  $r_1, r_2, \dots, r_p$ , in this layer are referred to as the consequent parameters.

**Layer 5:** It is a single fixed node and produces the overall output as the summation of contribution from each rule. This neuron calculates the sum of outputs of all defuzzification neurons and produces the overall ANFIS output

$$O'_5 = \sum_i O'_{4i} \quad (16)$$

Where  $O_{4i}$  output of layer4

### 3.2 Adaptive Neuro-Fuzzy principle and learning algorithm

Basically, ANFIS takes the initial fuzzy model and tunes it by means of a hybrid technique combining gradient descent back-propagation and mean least-squares optimization algorithms which are shown in Figure 7. The gradient descent algorithm is mainly implemented to tune the non-linear premise parameters and the least-square method is used to optimize or adjust the linear consequent parameters. At each epoch an error measured that defines the sum of the squared difference between actual and desired output. Training stops when either the predefined epoch number or error rate is obtained.

#### 3.2.1 Forward pass

In the forward pass, a training set of input patterns [as input vectors i.e  $V_{ds}$  and  $V_{qs}$ ] is presented to the ANFIS, node outputs are calculated on layer by layer basis, and rule consequent parameters are identified by the least-squares estimator. In the Takagi Sugeno type fuzzy inference, an output vector, duty ratio, is a linear function. Thus, given the values of the membership parameters (for example triangular MF which has 3 parameters  $a$ ,  $b$  and  $c$ ) and a training set of 10000 input [ $V_{ds}$  and  $V_{qs}$ ] and output [ *duty ratio*] patterns, one can form 10000 linear equations in terms of the consequent parameters ( $p$ ,  $q$  and  $r$ ) as:

$$\left. \begin{aligned}
 D_1(1) &= \overline{w}_1(1) [p_1 V_{ds}(1) + q_1 V_{qs}(1) + r_1] \\
 &\quad \overline{w}_2(1) [p_2 V_{ds}(1) + q_2 V_{qs}(1) + r_2] + \dots + \\
 &\quad \overline{w}_n(1) [p_n V_{ds}(1) + q_n V_{qs}(1) + r_n] \\
 D_p(2) &= \overline{w}_1(2) [p_1 V_{ds}(2) + q_1 V_{qs}(2) + r_1] \\
 &\quad \overline{w}_2(2) [p_2 V_{ds}(2) + q_2 V_{qs}(2) + r_2] + \dots + \\
 &\quad \overline{w}_n(2) [p_n V_{ds}(2) + q_n V_{qs}(2) + r_n] \\
 &\quad \cdot \\
 &\quad \cdot \\
 &\quad \cdot \\
 D_1(m) &= \overline{w}_1(m) [p_1 V_{ds}(m) + q_1 V_{qs}(m) + r_1] \\
 &\quad \overline{w}_2(m) [p_2 V_{ds}(m) + q_2 V_{qs}(m) + r_2] + \dots + \\
 &\quad \overline{w}_n(m) [p_n V_{ds}(m) + q_n V_{qs}(m) + r_n]
 \end{aligned} \right\} \quad (17)$$

Where  $m$  = input/output patterns;

$n$  = number of nodes in the rule layer = 25

$D_{1-p}$  the predicted duty ratio of the ANFIS when inputs  $V_{ds}$  and  $V_{qs}$  are presented to it.

Equation (24) can be written in a matrix form, such as

$$D_{1-p} = A k \quad (18)$$

Where  $D_{1-p}$  is a  $m \times 1 = 10000 \times 1$  predicted duty ratio vector

$$D_{1-p} = \begin{bmatrix} D_{1-p}(1) \\ D_{1-p}(2) \\ \vdots \\ D_{1-p}(m) \end{bmatrix} \quad (19)$$

**A** is a  $m \times n$  (1+ number of input variables) = 10000×75 matrix,

$$A = \begin{bmatrix} \bar{w}_1(1) & \bar{w}_1(1)V_{ds}(1) & \bar{w}_1(1)V_{qs}(1) & \dots & \bar{w}_n(1) & \bar{w}_n(1)V_{ds}(1) & \bar{w}_n(1)V_{qs}(1) \\ \bar{w}_1(2) & \bar{w}_1(2)V_{ds}(2) & \bar{w}_1(2)V_{qs}(2) & \dots & \bar{w}_n(2) & \bar{w}_n(2)V_{ds}(2) & \bar{w}_n(2)V_{qs}(2) \\ \vdots & \vdots & \vdots & \ddots & \vdots & \vdots & \vdots \\ \bar{w}_1(m) & \bar{w}_1(m)V_{ds}(m) & \bar{w}_1(m)V_{qs}(m) & \dots & \bar{w}_n(m) & \bar{w}_n(m)V_{ds}(m) & \bar{w}_n(m)V_{qs}(m) \end{bmatrix} \quad (20)$$

In this case, the number of input-output patterns  $m=10000$  used in training is greater than the number of consequent parameters  $n$  (1+ number of input variables) = 75. It means that we are dealing with an over-determined problem, and thus an exact solution to Equation (19) may not even exist. Instead, one should find a least-square estimate of  $k$ ,  $k^*$ , that minimizes the squared error medullas of  $\|Ak - D_{1-p}\|^2$ . This is achieved using the pseudo-inverse technique:

$$k^* = (A^T A)^{-1} A^T D_{1-p} \quad (21)$$

where  $A^T$  is the transpose of  $A$ , and  $(A^T A)^{-1} A^T$  is the pseudo-inverse of  $A$  if  $(A^T A)$  is non-singular. As soon as the rule consequent parameters are established, we can compute an actual network output vector  $D_1$ , and the error vector  $e$ , can be determined as,

$$e = D_{1-p} - D_1 \quad (22)$$

### 3.2.2 Backward pass

In the backward pass, the back-propagation algorithm is applied. The error signals are propagated back, and the antecedent parameters are updated according to the chain rule. For instance, consider a correction applied to parameter  $a$  of the bell-shaped membership function used in node  $A_j$ . The chain rule can be expressed from Equation (26) as,

$$\Delta a = -\eta \frac{\partial E}{\partial a} = -\eta \frac{\partial E}{\partial e} \times \frac{\partial e}{\partial D_1} \times \frac{\partial D_1}{\partial(\bar{w}_i f_i)} \times \frac{\partial(\bar{w}_i f_i)}{\partial \bar{w}_i} \times \frac{\partial \bar{w}_i}{\partial w_i} \times \frac{\partial w_i}{\partial w_{A_i}} \times \frac{\partial w_{A_i}}{\partial a} \quad (23)$$

Where  $\eta$  is the learning rate, and  $E$  is the instantaneous value of the squared error for the ANFIS output neuron, i.e.,

$$E = \frac{1}{2} e^2 = \frac{1}{2} (D_{1-p} - D_1)^2 \quad (24)$$

$$\Delta a = -\eta (D_{1-p} - D_1) (-1) f_i \times \frac{\bar{w}_i (1 - w_i)}{w_i} \times \frac{w_i}{w_{A_i}} \times \frac{\partial w_{A_i}}{\partial a} \quad (25)$$

Where

$$\frac{\partial w_{A_i}}{\partial a} = \frac{1}{\left[1 + \left(\frac{V_{ds} - a}{c}\right)^{2b}\right]^2} \times \frac{1}{c^{2b}} \times 2b \times (V_{ds} - a)^{2b-1} \times (-1) = w_{A_i}^2 \times \frac{2b}{c} \times \left(\frac{V_{ds} - a}{c}\right)^{2b-1} \quad (26)$$

Similarly, the corrections applied to parameters  $b$  and  $c$  can also be obtained.

#### 4. Results and Discussion

As explained in the previous section ANFIS based SVM is trained in under modulation region for equal two-level duty ratios and two-level index. From the obtained two-level duty ratios switching pulses  $S_a$ ,  $S_b$ ,  $S_c$  are generated using the switching frequency 3 kHz. The training data for ANFIS is generated by simulating the conventional SVM. The training time for one epoch is typically 5-10 minutes with 160GHz Pentium dual core PC and training error obtained is less than 0.0002. The number membership functions for the input variables d-axis- $V_{ds}$  and q-axis- $V_{qs}$  is 5 and 5 respectively. Therefore the number of rules is 25( $5*5=25$ ). Bell shape membership functions are used for two input variables  $V_{ds}$  and  $V_{qs}$ . Usually Bell shape membership function is specified by three parameters. Therefore ANFIS used here contains a total of 105 fitting parameters, of which 30( $5*3+5*3=30$ ) are premise parameters and 75( $3*25=75$ ) are consequent parameters.

From the obtained two-level switching pulses and two-level index, three-level switching pulses are generated by comparing two-level pulses with three-level switching pulses. These three-level switching pulses are fed to the inverter circuit.

##### 4.1 Performance of Induction motor at 3KHz inverter switching frequency

The performance of induction motor during starting and steady state with conventional and ANFIS based SVM methods at 3KHz inverter switching frequency and 400V DC link voltage is shown in Figure 8. It is observed that the speed response reaches the steady state earlier with ANFIS based SVM method compared to conventional based SVM method. The %THD of phase currents with conventional and ANFIS are shown in Figure 9.

The dynamic performance of induction motor drive for the step change in the load torque (15N-m) is shown in Figure 10. The torque ripple is less with ANFIS based SVM compared to neural and conventional based SVM methods. Due to this smooth speed response is obtained with ANFIS based SVM

##### 4.2 % THD of inverter Line voltages at 3 KHz switching frequency

The % THD of inverter line-line voltage with inverter DC voltage 150V and at switching frequency 3 KHz is as shown in the Figure 11. The %THD is less with ANFIS based SVM method compared to conventional SVM method.

##### 4.3 Comparison of THD at various switching frequencies:

The %THD values of three-level inverter line-line voltages ( $V_{ab}$ ,  $V_{bc}$  and  $V_{ca}$ ) at 3 kHz up to 50- harmonic order range with Conventional and ANFIS based SVM methods is as given in Table 2.

#### 5. Conclusion

An Adaptive Neuro-fuzzy based space vector modulation technique for a three-level inverter has been presented that operates in the under modulation region. The proposed Adaptive Neuro-Fuzzy based SVM method can be applied at any switching frequency. The duty ratios are generated independent of switching frequency. The Adaptive Neuro-fuzzy based SVM is simulated with the induction motor drive and evaluated thoroughly for steady state and dynamic performance with a conventional SVM. The performance of ANFIS based SVM is found to be excellent compared to the conventional based SVM method. The torque ripple is less with ANFIS based space vector modulation technique. Due to this smooth speed response obtained compared to conventional SVM method. The THD reduced by 40% with Adaptive Neuro Fuzzy based SVM method compared to conventional SVM.

#### Appendix

Machine rating= 3 hp

Parameters:

Stator resistance  $R_s=0.55\Omega$ , Stator inductance  $L_s=93.38\text{mH}$

Rotor resistance  $R_r=0.78\Omega$ , Rotor inductance  $L_r=93.36\text{mH}$

Magnetising inductance  $L_m=90.5\text{mH}$

Moment of inertia  $J=0.019\text{Kg-m}^2$ , Damping coefficient  $B=.000051$

**References**

Anshuman, Tripathi., Ashwin M. Khambadkone., and Sanjib K. Panda., (2005). Torque Ripple Analysis and Dynamic Performance of a Space Vector Modulation Based Control Method for AC-Drives. *IEEE Trans. Power. Electron.*, 20(2), 485-492.

Attainese.C, Nardi .V, and Tomasso.G., (2007 ).Space vector modulation algorithm for power losses and THD reduction in VSI based drives. *Electrical power components and systems*, 35(1), 1271-1283.

Jyh-Shing Roger Jang.,(1993). ANFIS : Adaptive-Network-Based Fuzzy Inference System. *IEEE Trans. Systems, man, and Cybernet.* 23( ),

Kwasinski. A, Krein P. T., and Chapman P. L., (2003). Time domain comparison of pulse-width modulation schemes. *IEEE Power Electron Lett.*, 1( 3), 64–68.

Mondal, K., Pinto, O.P., and Bimal K.Bose, (2002). A neural network based space vector PWM controller for a three level voltage-fed inverter induction motor drive. *IEEE Trans. Ind. Applicat.*, 38(3), 660–669..

Muthuramalingam, A., Sivaranjani, D.,and S.Himavathi, S., (2005). Space vector modulation of a voltage fed inverter using artificial neural networks. in proc. Conf IEEE Indicon, 487-491.

Pinto, J. O. P., Bose, B. K., L. Silva, L. E. B., and Kazmierkowski, M. P., (2000). A neural network based space vector PWM controller for voltage-fed inverter induction motor drive. *IEEE Trans. Ind. Applicat.*, 36(6), 1628–1636.

Wenxi, Yao., Haibing Hu., and Zhengyu Lu., (2008). Comparisons of space-vector modulation and carrier-based modulation of multilevel inverter. *IEEE Trans. Power. Electron.*, 23(1),45-51.



**G.Durgasukumar** received Bachelor's and Master's degrees in Electrical Engineering from J.N.T.U, Hyderabad (India) and pursuing his Ph.D.degree in the Electrical Engineering Dept, Indian Institute of Technology, Roorkee, India. His research interests include power electronics and electric drives, machines. He is presently pursuing Ph.D under the guidance of M.K.Pathak.



**Mukesh Kumar Pathak** was born in Hamirpur (HP), India, in 1966. He did his graduation in Electrical Engineering from L.D. Engineering College, Ahmedabad (Gujarat), India, in 1986. He joined Electrical Engineering Department of NIT, Kurukshetra (Haryana), India, as a Lecturer in 1987. In 1989 he joined Electrical Engineering Department of NIT, Hamirpur (HP), India, where he served till 2007. Presently, he is working as an Assistant Professor in Electrical Engineering Department of IIT Roorkee, India, where he joined in 2007. He obtained both his M.Tech (Power Electronics, Electrical Machines and Drives) and Ph.D. degrees from IIT Delhi, India. He has co-authored a book on Electric Machines. He is a member of IEEE, Life Fellow of Institution of Engineers (India), Life member of Indian Society for Technical Education (ISTE) and Systems Society of India (SSI).

Table 1. d and q components of the reference voltage  $V^{2*}$

S	$V_d^{2*}$	$V_q^{2*}$
1	$V_d^* - 2V \cdot \cos(0)$	$V_q^* - 2V \cdot \sin(0)$
2	$V_d^* - 2V \cdot \cos(\pi/3)$	$V_q^* - 2V \cdot \sin(\pi/3)$
3	$V_d^* - 2V \cdot \cos(2\pi/3)$	$V_q^* - 2V \cdot \sin(2\pi/3)$
4	$V_d^* - 2V \cdot \cos(\pi)$	$V_q^* - 2V \cdot \sin(\pi)$
5	$V_d^* - 2V \cdot \cos(4\pi/3)$	$V_q^* - 2V \cdot \sin(4\pi/3)$
6	$V_d^* - 2V \cdot \cos(5\pi/3)$	$V_q^* - 2V \cdot \sin(5\pi/3)$

Table 2. THD values of inverter Line-line Voltages

Switching frequency	parameter	Simulation	
		Conventional	ANFIS
3 kHz	$V_{ab}$	8.71	5.13
	$V_{bc}$	9.41	6.17
	$V_{ca}$	8.69	5.14

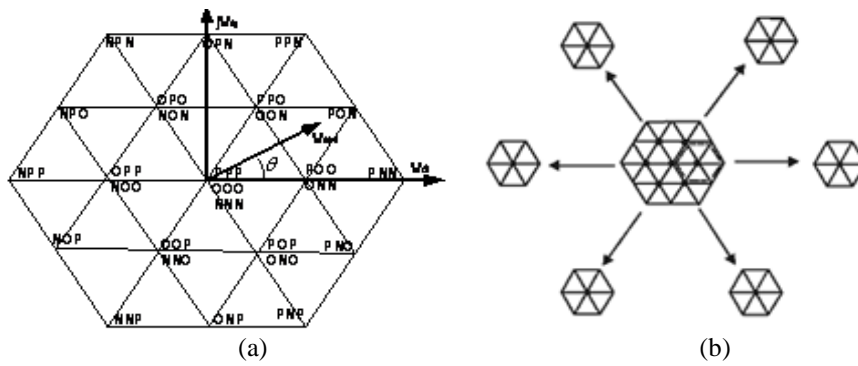


Figure 1. Space vector diagram of three-level inverter and six two-level hexagons

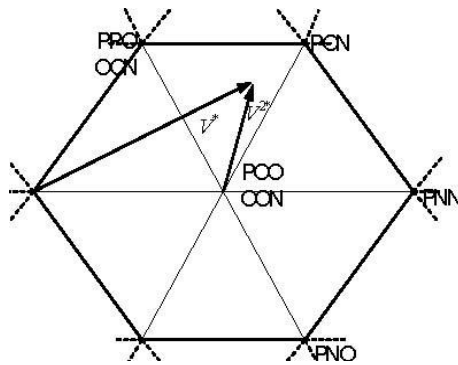


Figure 2. Change of original reference voltage vector

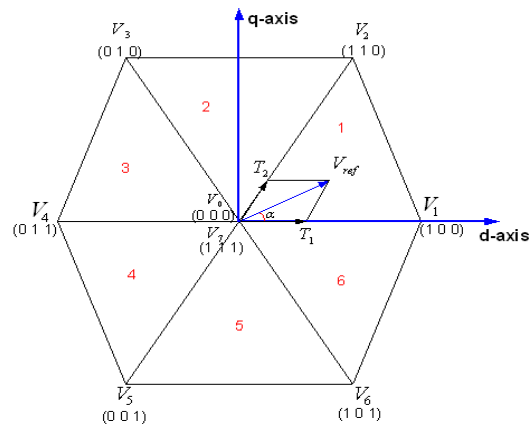


Figure 3. Two-level inverter Space vector diagram with active vectors

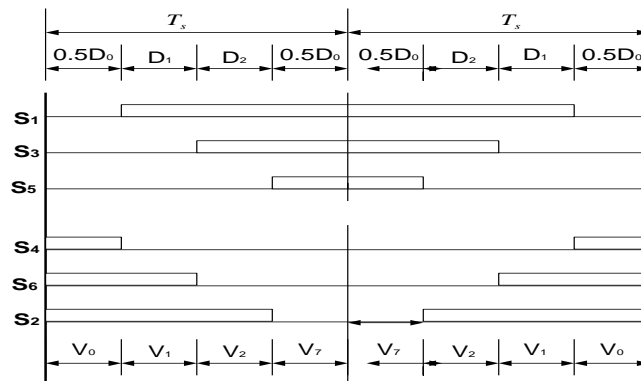


Figure 4. Actual gating signal pattern of the space vector PWM (in the case of the sector -1)

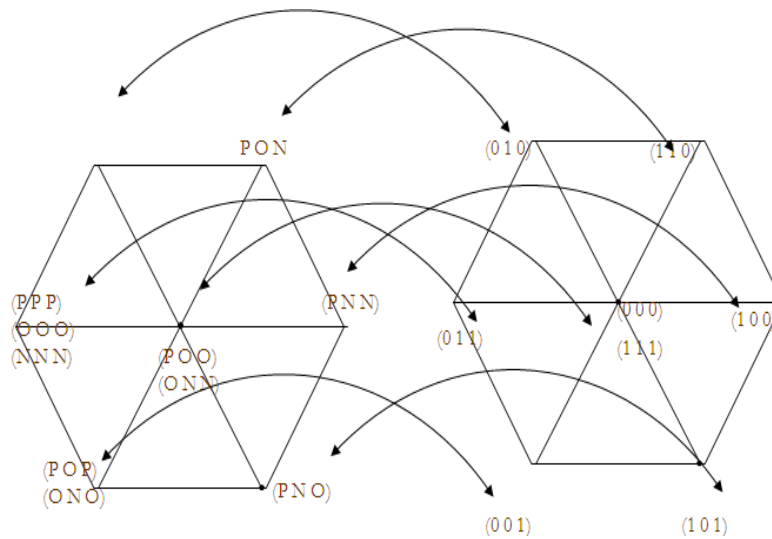


Figure 5. Conversion of Two-Level Switching States to Three Level Switching States

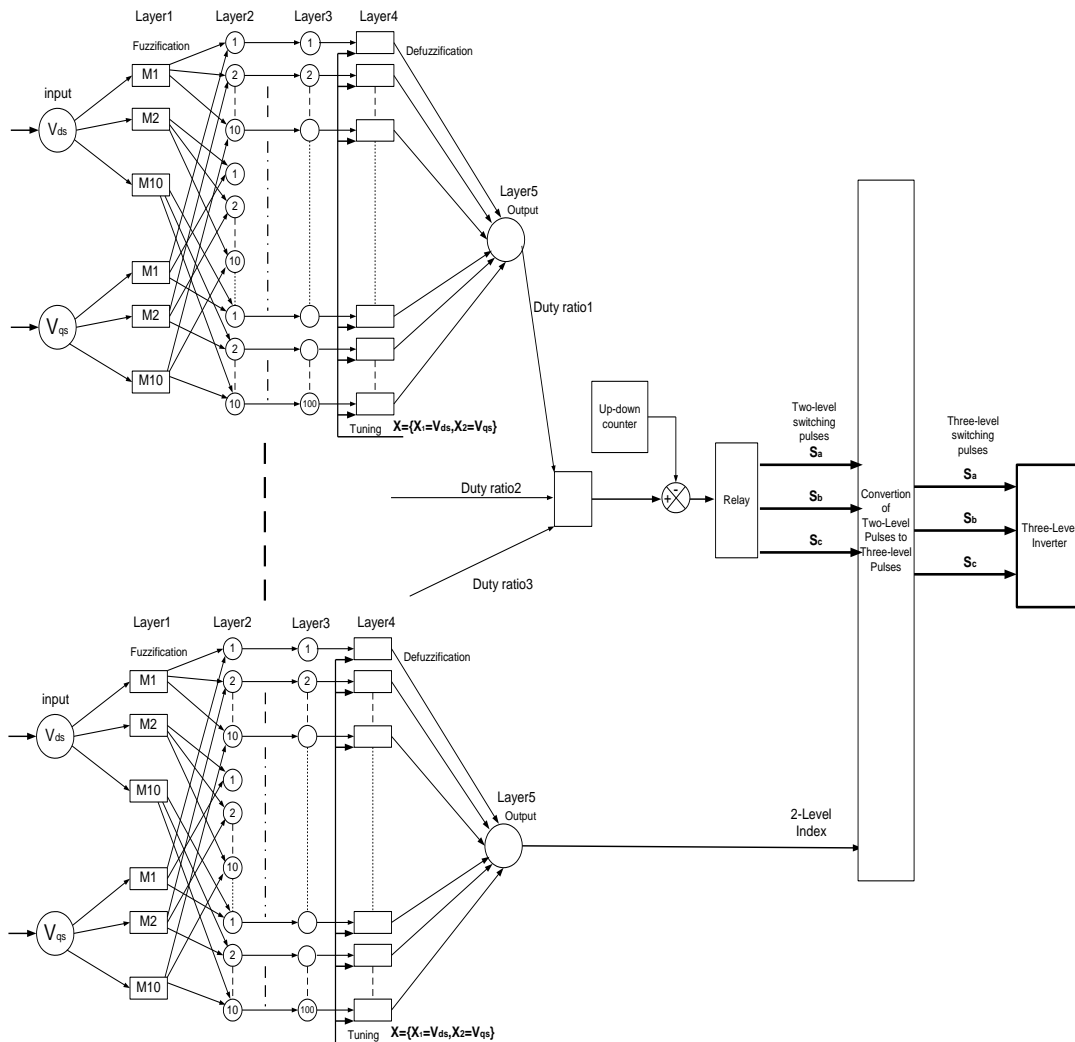


Figure 6. Structure of ANFIS for SVM

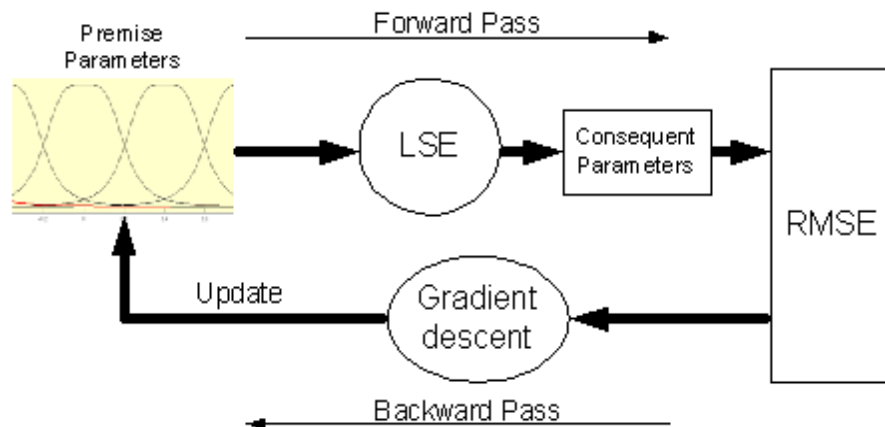


Figure 7. Anfis Hybrid learning algorithm

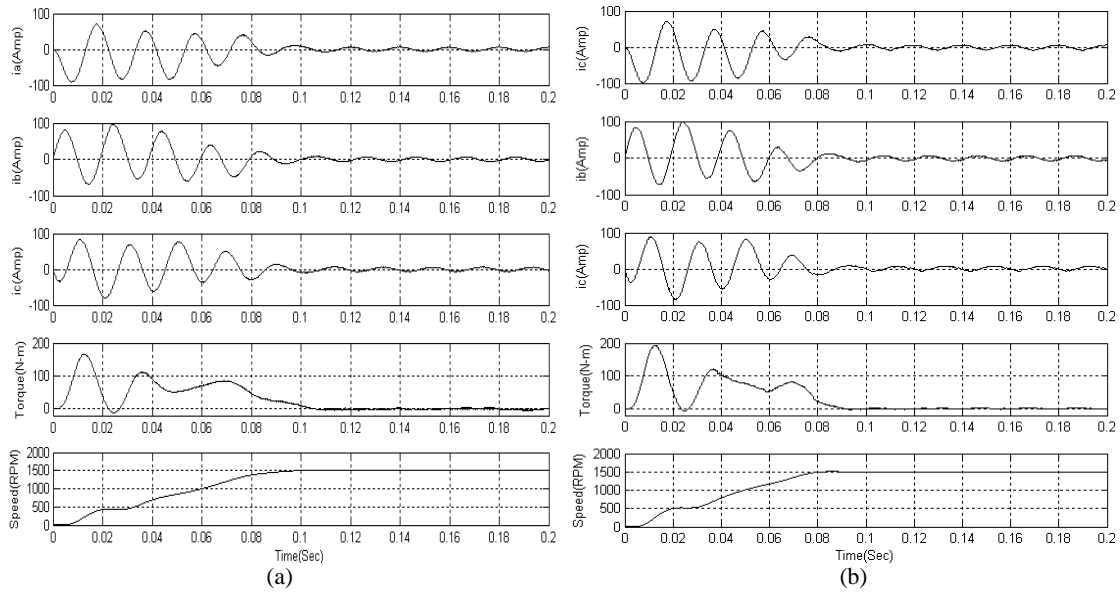


Figure 8. Performance of induction motor at 3KHz with a)Conventional SVM b) ANFIS SVM

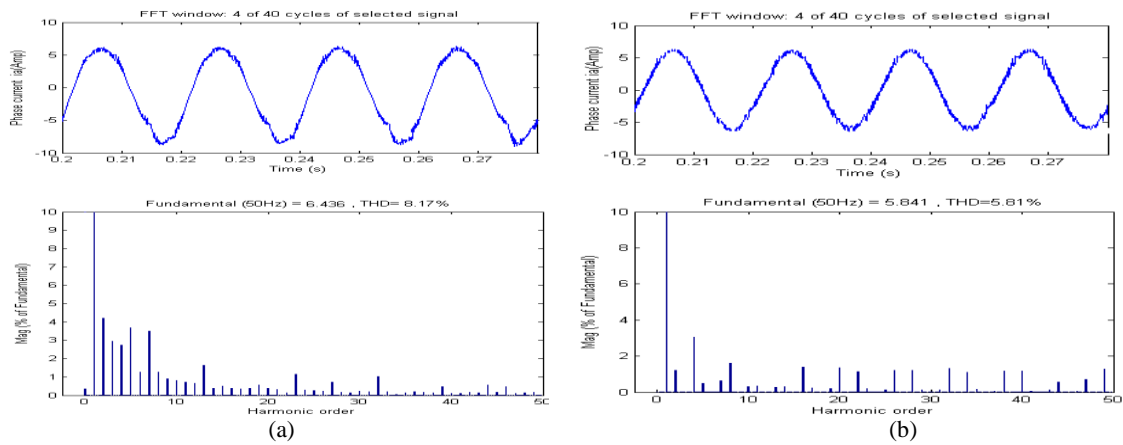


Figure 9. %THD of phase currents at 3KHz with a)Conventional SVM b) ANFIS SVM

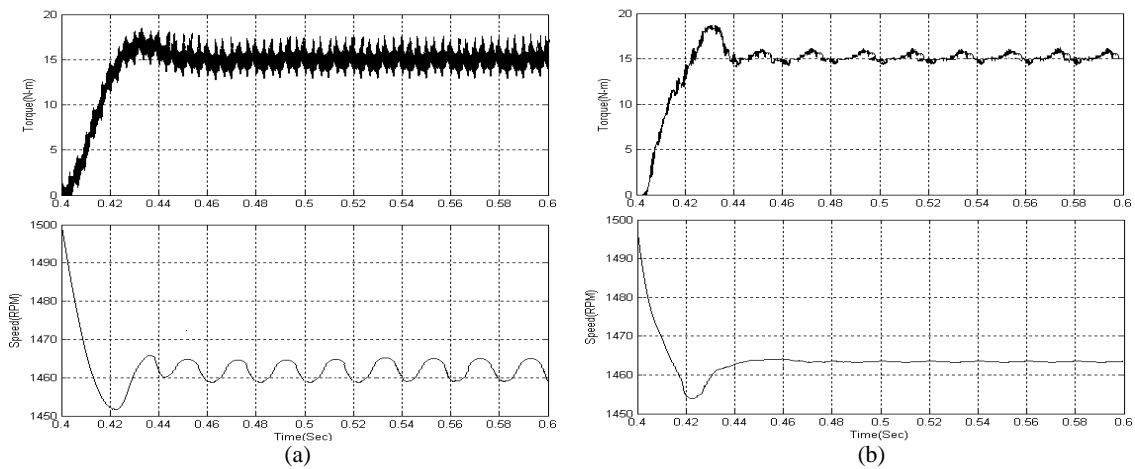


Figure 10. Performance during step change in load torque with a) Conventional SVM b)ANFIS SVM

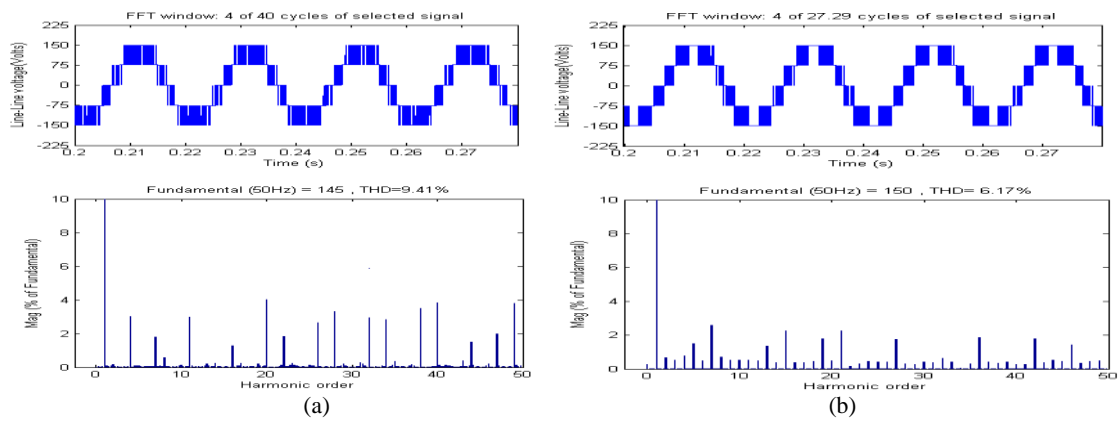


Figure 11. %THD of line-line at 3KHz inverter switching frequency with a)Conventional SVM b)ANFIS SVM

This academic article was published by The International Institute for Science, Technology and Education (IISTE). The IISTE is a pioneer in the Open Access Publishing service based in the U.S. and Europe. The aim of the institute is Accelerating Global Knowledge Sharing.

More information about the publisher can be found in the IISTE's homepage:

<http://www.iiste.org>

The IISTE is currently hosting more than 30 peer-reviewed academic journals and collaborating with academic institutions around the world. **Prospective authors of IISTE journals can find the submission instruction on the following page:**

<http://www.iiste.org/Journals/>

The IISTE editorial team promises to review and publish all the qualified submissions in a fast manner. All the journals articles are available online to the readers all over the world without financial, legal, or technical barriers other than those inseparable from gaining access to the internet itself. Printed version of the journals is also available upon request of readers and authors.

### **IISTE Knowledge Sharing Partners**

EBSCO, Index Copernicus, Ulrich's Periodicals Directory, JournalTOCS, PKP Open Archives Harvester, Bielefeld Academic Search Engine, Elektronische Zeitschriftenbibliothek EZB, Open J-Gate, OCLC WorldCat, Universe Digital Library, NewJour, Google Scholar

